Research Square

Preprints are preliminary reports that have not undergone peer review.
They should not be considered conclusive, used to inform clinical practice,
or referenced by the media as validated information.

Geological Modeling and In-situ Stress Field Simulation of Jurassic Unconventional Oil Reservoirs in the Sichuan Basin

Qingsong TANG
PetroChina Southwest Oil and Gasfield Company
Runfeng SHI
shirunfeng20021125@163.com
Southwest Petroleum University SWPU: Southwest Petroleum University https://orcid.org/0009-0009-7701-7357
Zhongbao WU
PetroChina Research Institute of Petrol Exploration and Production: Research Institute of Petroleum Exploration and Development https://orcid.org/0009-0007-9100-3790
Bing HE
Sichuan Oil Bureau: PetroChina Southwest Oil and Gasfield Company
Houbin LIU
Southwest Petroleum University SWPU: Southwest Petroleum University
Benjian ZHANG
PetroChina Southwest Oil and Gasfield Company
Minglei WANG
PetroChina Research Institute of Petrol Exploration and Production: Research Institute of Petroleum Exploration and Development
Xun ZHU
PetroChina Southwest Oil and Gasfield Company
Kai YU
PetroChina Southwest Oil and Gasfield Company
Huizhu XIANG
PetroChina Research Institute of Petrol Exploration and Production: Research Institute of Petroleum Exploration and Development

Research Article

Keywords: geology-engineering integration, lithofacies model, structural model, property model, in-situ stress model

Posted Date: November 23rd, 2026

DOI: https://doi.org/10.21203/rs.3.rs-11036088/v1

License: This work is licensed under a Creative Commons Attribution 4.0 International License.
Read Full License

Geological Modeling and In-situ Stress Field Simulation of Jurassic Unconventional Oil Reservoirs in the Sichuan Basin

Qingsong TANG[a],Runfeng SHI[b],Zhongbao WU[c*],Bing HE[c],Houbin LIU[b],Benjian ZHANG[a],Minglei WANG[c],Xun ZHU[a],Kai YU[a] and Huizhu XIANG[c]

[a]*Petro China Sounthwest Oil & Gasfiled Company, Chengdu, China;*[b]*State Key Laboratory of Oil and Gas Reservoir Geology and Exploitation, Southwest Petroleum University,* [c]*Research Institute Of Petroleum Exploration & Development, Beijing, China*

Author Profile: Qingsong TANG (1981—), male, born in Guang'an, Sichuan Province. Senior Engineer, Master's degree. His research focuses on development geology and management. Address: No. 3, Section 1, Fuqing Road, Chenghua District, Chengdu, Sichuan Province 610051, China. E-mail: Tangqingsong2008@petrochina.com.cn

Zhongbao WU*:wzbwxl@sina.com

Geological Modeling and In-situ Stress Field Simulation of Jurassic Unconventional Oil Reservoirs in the Sichuan Basin

Abstract: Aiming to address complex geological conditions, difficulties in collaborative multi-parameter characterization, and insufficient in-situ stress prediction accuracy for Jurassic unconventional oil reservoirs in the Sichuan Basin, this study adopts an integrated modeling framework of "structure control–lithofacies constraint–property characterization–in-situ stress modeling" using professional geological software. Multi-source geological data are integrated to construct structural, lithofacies, reservoir property, and in-situ stress models, establishing a three-dimensional geological model and verifying its accuracy. Results show that structural geometry is governed by regional tectonic movements, lithofacies distribute in a banded pattern, and reservoir properties exhibit significant spatial heterogeneity. The in-situ stress field correlates strongly with structural geometry and lithofacies, with the maximum principal stress orientation consistent with the regional structural trend. This integrated method effectively improves geological characterization precision and overcomes limitations of traditional approaches. The findings provide a scientific basis for exploration, development, and reservoir stimulation design of Jurassic unconventional oil reservoirs, offering valuable references for modeling similar continental unconventional oil reservoirs.

Key words: geology-engineering integration, lithofacies model, structural model, property model, in-situ stress model

1 Introduction

As an important birthplace and strategic base for China's oil and gas industry, the Sichuan Basin is a typical large superimposed petroliferous basin in terms of geological structure [HUANG Dong, et al.2017]. The basin has huge potential for tight oil and gas resources. These resources are mainly

concentrated in the Upper Triassic and Jurassic strata [ZHANG Daowei, et al.2022]. Due to multiple expansions and vertical superimpositions of the lake basin during the Jurassic period, multiple sets of high-quality source rocks developed. Currently, five major oil-bearing series have been identified vertically. They are: the Shaximiao Formation, Lianggaoshan Formation, and the Da'anzhan, Dongyuemiao, and Zhenzhuchong members of the Ziliujing Formation [QIAO Ling,2013]. The Shaximiao Formation, with widely distributed channel sand bodies, source faults, and excellent caprock, is the main battlefield for tight oil exploration and development [LIAO Guangzhi,et al.2025][YAN Xueying, et al.2024]. Due to the strong heterogeneity and complex spatial distribution of tight oil and gas reservoirs in this area, exploration and development are difficult. Accurate geological modeling is a key link connecting geological research and engineering practice. Precisely constructing a geological model directly determines the scientific nature of reservoir evaluation and the rationality of development plans. It is an important prerequisite for achieving efficient and precise development of tight oil and gas resources in this area.

Traditional methods of lithology classification using property thresholds often result in lithofacies models that differ greatly from reality. This paper uses a method combining well and seismic data. It combines vertical and horizontal distribution probability with trend surface methods to build a lithofacies model. Comparison and verification show that this lithofacies model accurately restores the spatial distribution characteristics of channel sand bodies. The model accuracy meets geological understanding. It provides reliable spatial constraints for subsequent facies-controlled property modeling. For the in-situ stress model, A scholar [HUANG Rongzun.1981] established a mathematical model for underground in-situ stress. He used logging information to determine parameters. However, this model

did not consider the influence factors of Young's modulus. A scholar [WANG Xiuchao.2018] established a Suárez-Rivera in-situ stress calculation model based on transversely isotropic media. In addition, Some scholars [JIA Lichun,et al.2023] combined experimental and logging interpretation results. They built a multi-parameter formation pore pressure prediction model for carbonate formations based on Terzaghi's effective stress theory. Some scholars [JIANG Xiaohong, et al.2016] used logging data to calculate the three-pressure data for the GM block. Some scholars [Liu Qiming et al.2017] established the three-pressure profile for the Pengzhou block. They analyzed the reasons for complex formation pressure. Some scholars [Fan Yu et al.2023] comprehensively used theoretical research and engineering geological information analysis methods. They established a scientific and reasonable prediction model for abnormal high pressure in sandstone-mudstone and carbonate formations in the Penglai gas area. They constructed a full-wellbore formation pressure vertical distribution profile for the Penglai gas area. Some scholars [Chen Ming et al.2021] proposed a new formation pressure prediction method. It overcomes problems such as poor quality of shallow interval transit time curves. A scholar [Liu Ying.2021] used actual drilling data to predict formation pressures and conduct wellbore stability analysis for the Taihudongmiao Member in the Fuxing area. Some scholars [Zhao Xuyang et al.2021] used improved shear wave to predict in-situ stress and rock mechanical parameters for the block. Some researchers [Chen Ke et al.2023] established a stress field model near faults. Finally, after comparison and selection, based on rock mechanical parameter modeling, this study used some empirical coefficients for certain parameters. The "constant strain coefficient" method was used to estimate the magnitudes of the maximum and minimum horizontal principal stresses. Comparison with actual data shows a match rate of over 90%. This provides a scientific basis for oil and gas exploration, development planning, and

reservoir stimulation design in the Shaximiao Formation. It offers valuable references for modeling similar continental sandstone reservoirs.

2 Detailed Geological Structural Characterization of the Reservoir

2.1 Block Geological and Engineering Situation

The study area is located in Nanchong City, Sichuan Province. It belongs to the northern part of the low-gentle belt in the Central Sichuan Paleouplift. This structural belt is adjacent to the low-gentle belt of the North Sichuan Paleodepression to the north and the low-steep belt of the West Sichuan Mesodepression to the south. It is next to the high-steep fault-fold belt of the East Sichuan Paleoslope to the east. The study area is in the northeastern part of central Sichuan. The elevation ranges from 330 to 440 m. The terrain is high in the northeast and low in the southwest. The study area is located in the Central Sichuan Paleouplift gentle structural area and the North Sichuan Paleodepression gentle structural area. Surface structures are gentle with simple morphology. Structures are relatively developed. The overall structural trend is a plunging monocline folding from south to north. Local structural traps develop. The Shuanghechang structure develops in the north. The Nanchong and Dacheng structures develop in the south. The Gongshanmiao structure develops in the west. The Yingshan structure develops in the east [LI Xiuming, et al.2022]. A large number of small-scale normal faults develop on the surface. These faults do not destroy the integrity of the surface structure.

Within the Shaximiao Formation, the top of a ~3–5 m thick greenish-gray or gray-black "Estheria shale" serves as a layering marker. This further divides the Shaximiao Formation into the first

and second members. The top boundary of the Shaximiao-1 Member, the Estheria shale layer, is visible inside the oilfield. In other areas, division is based on electrical characteristics [YANG Yu,et al.2023].

2.2 Reservoir Fracture System Identification and Construction

2.2.1 Fault Identification Based on Seismic Data

Based on multi-attribute collaborative analysis of post-stack 3D seismic data volumes, we initially defined the boundary characteristics and geometric attributes of faults and folds. On this basis, we used a human-computer interactive interpretation mode. We traced faults segment by segment along seismic sections and attribute slices. We quantitatively extracted fault occurrence information (strike, dip). We measured their vertical throw and horizontal extension range. This established the spatial distribution pattern of faults. Then, we imported the interpretation data into the geological modeling system. We used spatial interpolation algorithms and gridding techniques to construct the 3D geometric model of large-scale faults. As shown in Figure 1, the main fault system identified by the model has high consistency with the regional geological structural background of the study area. There is one major fault in the block.

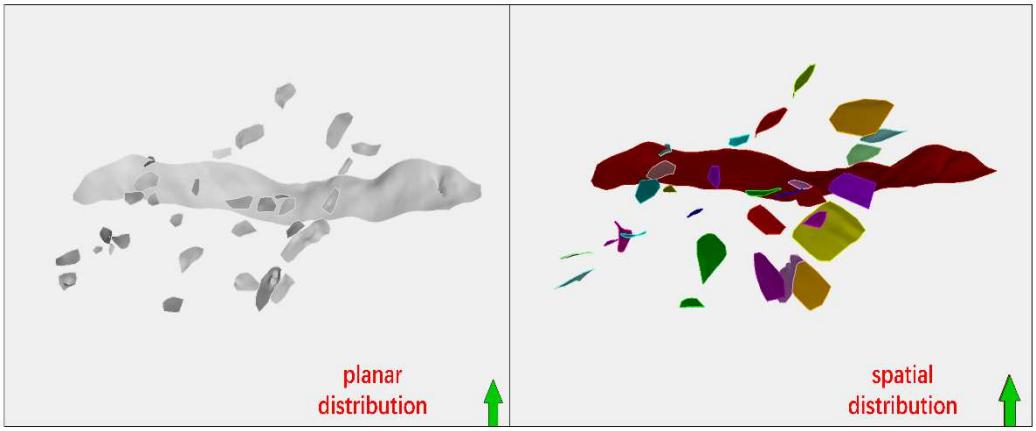

Figure 1. Fault plane and spatial distribution in the block

2.2.2 Fracture Identification Based on Ant Tracking Technology

Ant tracking technology is an automatic fracture extraction technology based on ant colony optimization algorithms [Stein Inge Pedersen.2002]. It simulates the collective behavior of ants foraging in nature. It intelligently traces discontinuous boundaries in 3D seismic data. It effectively solves problems of unclear fracture identification and poor continuity in low signal-to-noise ratio areas using traditional methods. This technology aims to finely identify medium and small-scale fractures. It quickly builds their geometric shape and distribution model. Its core workflow includes three main steps: from seismic data preprocessing to boundary detection and enhancement, and finally to fracture/fault extraction and interpretation. This quickly builds the fracture geometry and distribution model.

The seismic data preprocessing process includes: structural smoothing to remove random noise from the seismic data volume, enhancing data continuity and interpretability; amplitude contrast to detect amplitude changes at fault/fracture locations, highlighting interfaces with property changes in the formation, and showing fault/fracture details; 3D boundary enhancement to enhance fracture edge features and improve 3D structural boundary visibility in the data.

To further improve the accuracy and continuity of fracture identification, this study implemented a "fine parameter filtering combined with multi-iteration tracking" strategy after seismic data preprocessing. First, we used occurrence filtering to effectively suppress formation background interference: we set a dip angle threshold to filter out reflections from gentle formations with dips less than 45°, retaining high-angle structural fracture signals; we also set an azimuth condition to eliminate clutter signals with an angle greater than 45° from the main fault strike, enhancing the response along the dominant fault direction. Second, we used iterative tracking "from coarse to fine": the first round

used "passive mode" to initially extract backbone faults, ensuring the reliability of main fracture surfaces; then it switched to "active mode" to further extract and enhance the details and connectivity of micro-fractures while continuously suppressing low-dip noise. The dynamic evolution process of ant tracking is shown in Figure 2.

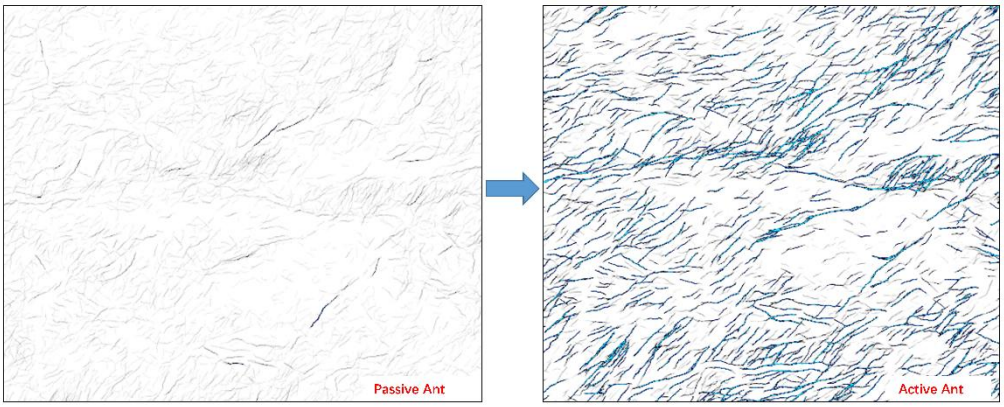

Figure 2. Multiple iterations of tracking

Finally, after multiple parameter adjustments and iterative calculations, we obtained a high signal-to-noise ratio fracture distribution result (as shown in Figure 3). This achieved a fine characterization of the overall medium and small-scale fracture system in the target area. Combined with the analysis of major faults interpreted manually (as shown in Figure 3), the structure in this study block is relatively gentle. Fracture distribution is relatively uniform and mainly concentrated near faults.

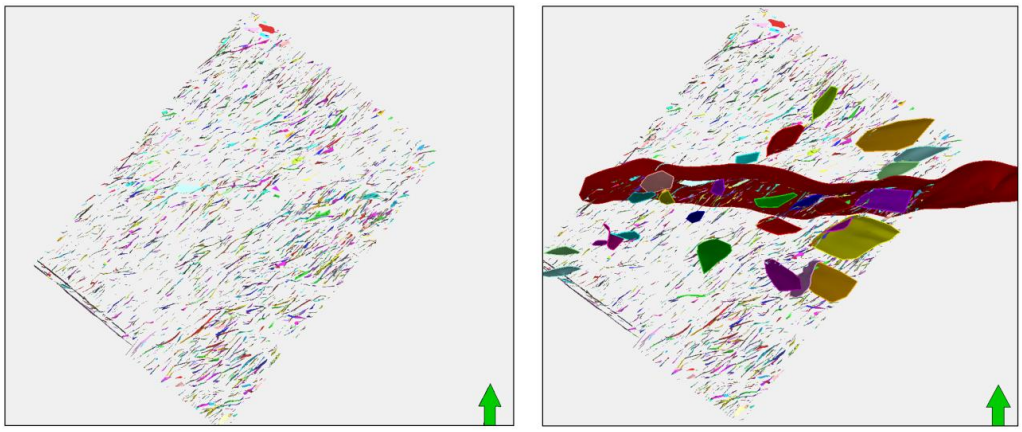

Figure 3. Ant tracking fracture distribution results and fault comparison

2.3 Study on Fine Characterization of Reservoir Lithofacies

2.3.1 Method for Fine Characterization of Reservoir Lithofacies Using Well-Seismic Integration

The accuracy of reservoir lithofacies identification directly determines the reliability of geological modeling. In actual exploration and development, logging data has very high vertical resolution. It can accurately identify lithology at the wellbore, but its lateral distribution is isolated. Seismic data has continuous lateral coverage, but its vertical resolution is low and it has ambiguity. Therefore, the core of well-seismic integration is using mathematical algorithms. It uses logging "hard data" as constraints or labels to correct and guide seismic "soft data" for spatial prediction. This overcomes the limitations of single data sources in scale and accuracy. The basis of well-seismic integration is rock physics analysis and horizon calibration. The primary prerequisite is establishing an accurate correspondence between well logs and seismic data. First, rock physical modeling is required. We correct for the influence of borehole environment on logging curves. We upscale logging data to the seismic scale to eliminate high-frequency noise interference. We analyze the sensitivity differences of different lithofacies in rock physical parameters. This provides a physical basis for subsequent identification. Second, we complete horizon calibration by making synthetic seismograms, as shown in Figure 4.

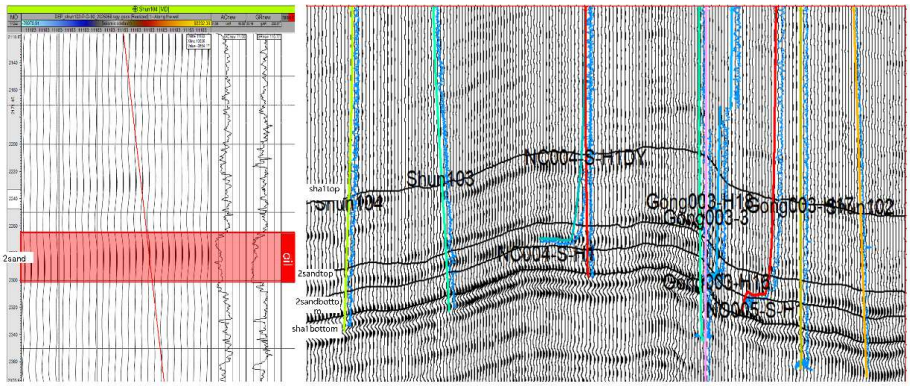

149

150 Figure 4. Well-seismic calibration chart

151 Analysis of the above figure shows that the oil layer obtained from logging interpretation
152 matches the low values of GR/AC curves. It corresponds to the medium-strong amplitude peak
153 characteristics in the seismic section. Therefore, we can determine the approximate distribution of
154 channel sand bodies through the medium-strong amplitude peak characteristics of seismic attributes.
155 Based on the actual data collection in the study block, this study uses a geostatistics-based co-simulation
156 method for well-seismic integrated lithofacies characterization: this method mainly uses the co-kriging
157 algorithm. It uses sparse well-point lithofacies data as the primary variable and dense seismic attributes
158 across the entire area as the co-variable. It analyzes the spatial variation structure of lithofacies through
159 variograms. While maintaining the accuracy of well-point data, it uses the lateral variation trend of
160 seismic attributes to guide inter-well interpolation.

161 *2.3.2 Construction of the Structural Model*

162 The core logic of 3D geological modeling is converting discrete geological horizon data into a continuous
163 3D spatial representation. This paper uses corner-point grid modeling technology. By defining the study
164 area boundary, we first build a 3D structural grid framework. We define the spatial extent and fault

constraint relationships of the study block. On this basis, we perform vertical layering according to formation interfaces and sedimentary characteristics. We build a 3D grid model reflecting reservoir structural characteristics. Through the above steps, we achieve a unified expression of the geological model from spatial structure to sequence division. This provides the basis for subsequent lithofacies modeling and property parameter assignment. The final 3D grid system consists of tens of millions of parameterized subdivision units. Each unit serves as a basic computational operator for spatial property filling and numerical simulation. Taking the study block as an example, the model's plane coverage is 25 km × 17 km. To balance computational efficiency for numerical simulation and accuracy requirements for geomechanical analysis, the grid step size is finely set to 50 m × 50 m × 1 m. This model generates a total of 38,358,768 grid units, forming a high-precision 3D geological structural model (as shown in Figure 5). This lays a solid data foundation for subsequent multi-field coupled numerical simulation. The figure shows that the formation in this study block has no obvious undulation characteristics, and the terrain is relatively flat. A major fault passes through the middle part of the block, with slight terrain relief at the fault.

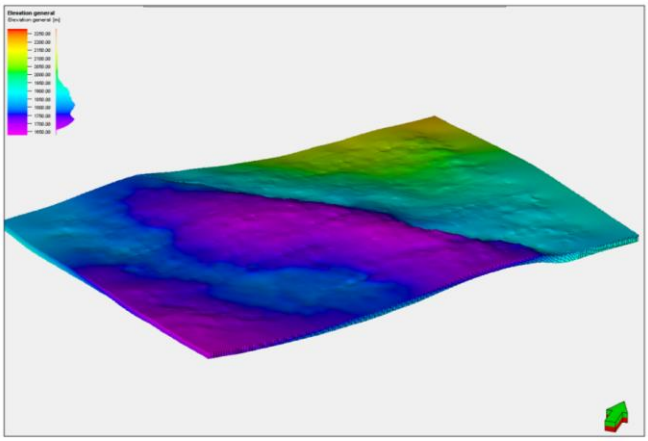

Figure 5. 3D Geological Structural Model

2.3.3 Construction of the Lithofacies Model

First, based on the structural model and the channel sand body range from logging interpretation, we generate a plane sedimentary facies map through horizon assignment. Using the lithofacies modeling module in geological modeling software, we use the assignment method to build a preliminary lithofacies model for the entire region. This determines the overall distribution range of sand bodies. We resample seismic inversion data to the structural grid. By comparing the channel connecting well sections of seismic inversion data with logging interpretation results, we determine the sand body threshold. This establishes a preliminary sedimentary facies model and exports the vertical distribution probability of sand bodies. At the same time, we generate a trend surface based on the channel range. Then, we upscale well logging lithofacies data. Controlled by the preliminary sedimentary facies model and using seismic data as a soft constraint, we comprehensively utilize the exported distribution probability and trend surface. We use the sequential indicator simulation method for constrained modeling. Finally, we obtain the block lithofacies model (Figure 6).

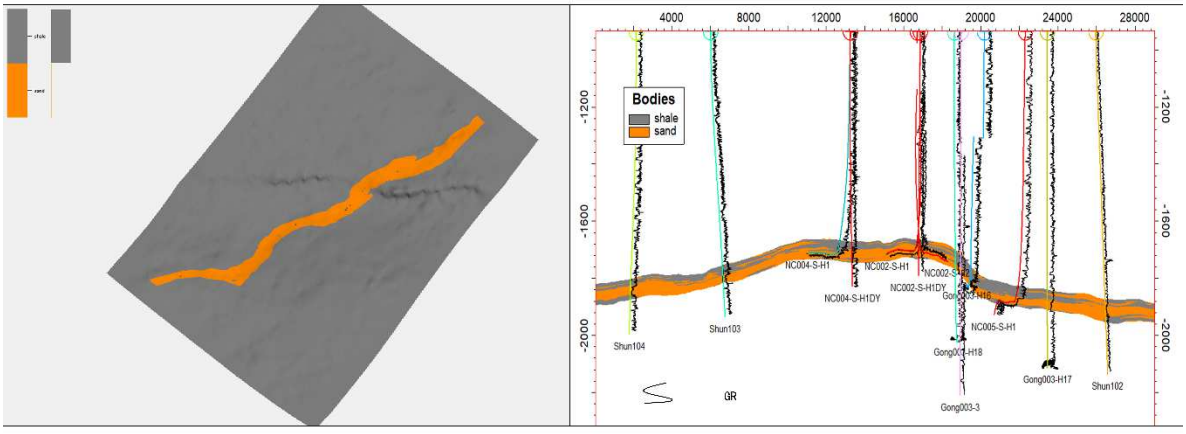

Lithofacies Model　　Vertical Distribution Map

Figure 6. Lithofacies Model and Vertical Distribution Map

Through systematic evaluation of the lithofacies model, we found: In terms of plane distribution, the lithofacies distribution range has high consistency with the sand body boundary range. In terms of vertical evolution, the sand body boundaries identified by the model precisely correspond to the low-value areas of the logging gamma ray curve. It effectively characterizes the cyclicity of the formation. Comparison and verification show that this lithofacies model accurately restores the spatial distribution characteristics of channel sand bodies. The model accuracy meets geological understanding. It can provide reliable spatial constraints for subsequent facies-controlled property modeling.

3 Reservoir 3D Property Parameter Modeling and Analysis

3.1 Single-Well Property Parameter Calculation

Aiming at the characteristics of the sandstone reservoir in the Shaximiao-1 Member of the Shaximiao Formation in the study block, this study used core-measured data to compare and select various property calculation models. The goal was to establish high-accuracy interpretation models for porosity, permeability, and saturation. This provides accurate basic data for subsequent reservoir property evaluation and rock mechanical parameter calculation.

(1) Porosity Calculation Model

For porosity calculation, the study compared the Wyllie time-average equation, the Raymer empirical equation, and the formation factor model. Comparing the calculation results of multiple models shows that the porosity model based on formation factor conversion has a higher correlation with core-

measured data. It can more truly reflect the pore space characteristics of low-porosity and low-permeability reservoirs.

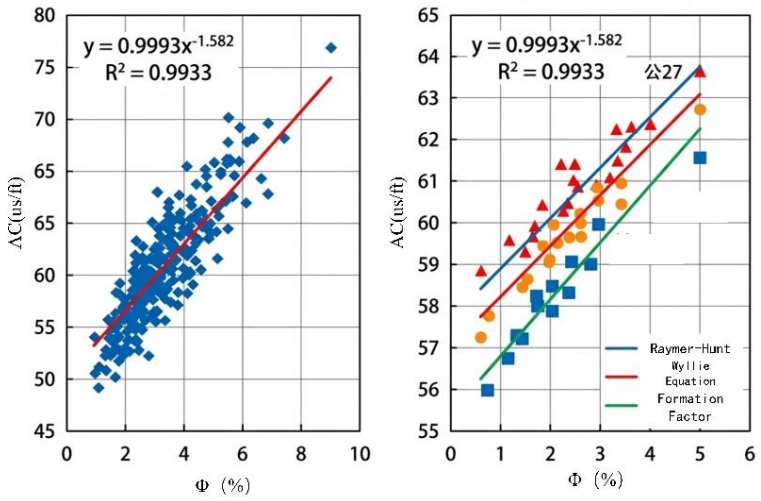

Figure 7. Porosity Calculation Model Selection (Left: Core porosity vs. acoustic crossplot; Right: Porosity calculated by various models)

(2) Establishment of Permeability Interpretation Model

Due to the strong heterogeneity of the reservoir in the Shaximiao-1 Member, permeability is controlled by complex factors. Based on eliminating fracture interference, this study focused on fitting analysis of the relationship between matrix porosity and permeability. Based on experimental results of sandstone porosity and permeability in the Shaximiao-1 Member, we established the following exponential relationship model:

$$K = 0.0026e^{3.0481\varphi} \quad (1)$$

The results are shown in Figure 8. This model has high reliability in predicting sandstone matrix permeability.

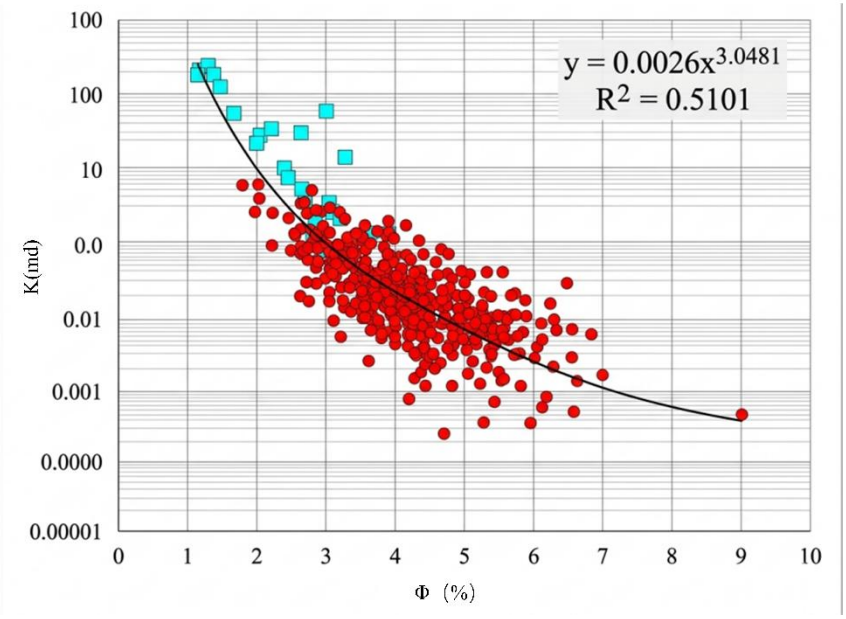

Figure 8. Porosity-Permeability Relationship Chart (fractures removed)

(3) Saturation Calculation

The Archie equation has wide applicability in fluid identification for sandstone-mudstone reservoirs. Based on the electrical characteristics of the sandstone reservoir in the Shaximiao Formation of the study area, its conductivity mechanism is mainly determined by the salinity of formation water and the complexity of pore structure. The calculation formula is shown in Equation 2:

$$S_w = \sqrt[n]{\frac{abR_w}{\varphi^m R_t}} \quad (1)$$

Where:a, b, m, n are rock electrical parameters, obtained from experiments in the previous section, R_w is formation water resistivity, R_t is formation resistivity.

Table 1. Rock-electric parameters and formation water resistivity for the Shaximiao-1 Member

Area	Layer	Sand Group / Reservoir Type	Rock-electric parameters				Formation Water Resistivity（Ω·m）
			a	b	m	n	Rw
G		Porous Type	0.999	1.207	1.582	2.598	0.06-0.08

	Shaximiao-1 Member	Fracture-Porous Type			1.5		

3.2 Establishment of Reservoir 3D Property Parameter Model

To truly characterize reservoir heterogeneity, this paper uses the sequential Gaussian simulation method to build the 3D property field. This effectively overcomes the "smoothing effect" of traditional interpolation algorithms. During the modeling process, we implemented a "well-constrained, seismic-guided" collaborative constraint strategy. We used well-point data as the primary variable. We introduced seismic inversion acoustic impedance, sedimentary facies, and structural trend surfaces as secondary information for joint solving. This ensures the property field balances microscopic accuracy and macroscopic geological laws. Based on this framework, we finally established the 3D multi-parameter static geological model for the Shaximiao-1 Member (Figures 9). The model results show that the porosity of channel sand bodies in the study area ranges from 4% to 8%. Permeability ranges from 0.01 to 3 mD. Water saturation ranges from 30% to 45%.

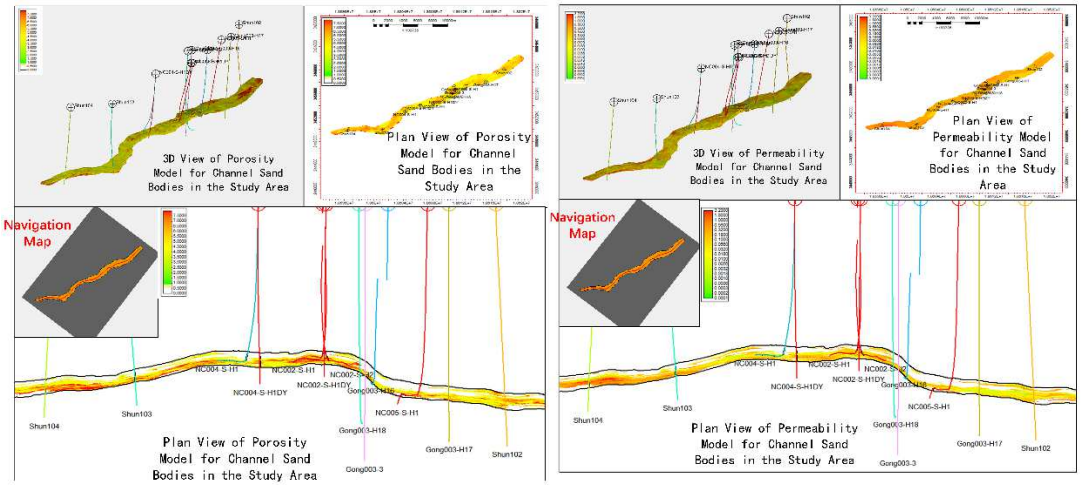

a b

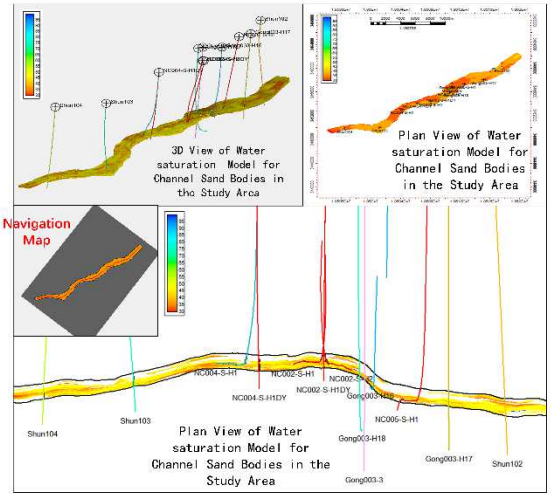

c

Fig. 9. Distribution of 3D static geological parameter models (a: Porosity, b: Permeability, c: Water saturation)

4 Reservoir 3D Geomechanical Modeling and Analysis

4.1 Single-Well Geomechanical Parameter Calculation

4.1.1 Single-Well Geomechanical Parameter Calculation Model

Using the compressional wave slowness Δt_P and shear wave slowness Δt_s from well logging, we calculate rock mechanical parameters and seepage property parameters using the following formulas.

Poisson's Ratio: $$\mu_d = \frac{\Delta t_S^2 - \Delta t_P^2}{2(\Delta t_S^2 - \Delta t_P^2)}, \mu_s = 2.623\mu^{2.100} \quad (3)$$

Elastic Modulus: $$E_d = \frac{\rho(3\Delta t_S^2 - 4\Delta t_P^2)}{\Delta t_S^2(\Delta t_S^2 - \Delta t_P^2)} \cdot a, E_s = 2.8156E^{0.8634} \quad (4)$$

Rock Shear Modulus: $$G = \frac{\rho}{\Delta t_S^2} \cdot a \quad (5)$$

Effective Stress Coefficient: $$\alpha_B = 1 - \frac{K}{K_s} \quad (6)$$

Cohesion: $$C = \frac{0.025E}{C_b}[8V_{cl} + 4.5(1 - V_{cl})] \times 10^{-3} \quad (7)$$

Compressive Strength: $$\sigma_c = \frac{2\cos\varphi}{1-\sin\varphi}C \quad (8)$$

Tensile Strength: $$\sigma_t = \sigma_c/12 \quad (9)$$

Where: μ_d, μ_s are dynamic and static Poisson's ratios of the rock, dimensionless, Δt_s, Δt_p are shear wave slowness and compressional wave slowness, μs/m, a is a unit conversion coefficient, varies with units, E_d, E_s are dynamic and static elastic moduli of the rock, MPa, ρis rock density, g/cm³, G K is rock bulk modulus, GPa, K is rock bulk modulus, GPa, K_s is rock grain bulk modulus, GPa, α_B is effective stress coefficient, dimensionless, C is cohesive strength, MPa, V_{cl} is shale content in the rock, dimensionless, σ_c, σ_t are uniaxial compressive strength and tensile strength of the rock, MPa, φis internal friction angle of the rock, °.

4.1.2 In-Situ Stress Calculation Model

(1) Vertical In-Situ Stress

It is generally believed that vertical in-situ stress equals the overburden pressure. Overburden pressure is the pressure on the formation caused by the total weight of the bedrock and fluids in the rock pores above a certain depth.

$$\sigma_v = \int_0^H \rho(h) g dh \quad (10)$$

(2) Maximum and Minimum Horizontal Principal Stresses

The Shaximiao Formation in the Sichuan Basin is under strong tectonic compression. The formation lithology shows typical interbedding of channel sand bodies and floodplain mudstone. This study uses the combined spring model to calculate horizontal principal in-situ stress. This model introduces the

controlling effect of Young's modulus (E) on the tectonic term. It can accurately characterize inter-layer differences in in-situ stress caused by sudden changes in rock mechanical parameters. This has important physical significance for evaluating fracture height extension during hydraulic fracturing in the Shaximiao Formation. The combined spring model formulas are as follows:

$$\sigma_H = \frac{\mu}{1-\mu}\sigma_v - \frac{\mu}{1-\mu}\alpha_B P_p + \frac{E}{1-\mu^2}(\varepsilon_H + \mu\varepsilon_h) + \alpha_B P_p \quad (11)$$

$$\sigma_h = \frac{\mu}{1-\mu}\sigma_v - \frac{\mu}{1-\mu}\alpha_B P_p + \frac{E}{1-\mu^2}(\varepsilon_h + \mu\varepsilon_H) + \alpha_B P_p \quad (12)$$

Where: σ_v, σ_H, σ_h are vertical, maximum horizontal, and minimum horizontal in-situ stresses, MPa, ε_h, ε_H are tectonic strains in the maximum and minimum horizontal principal stress directions, dimensionless.

4.1.3 Formation Pore Pressure Calculation Model

The Shaximiao-1 Member develops thick and stable purple-red mudstone. Its acoustic slowness evolution with depth has a good exponential decay law. This provides a rock physical basis for establishing a high-confidence normal compaction trend line. Compared to the high sensitivity of the effective stress method to mechanical parameters like Biot's coefficient, the Eaton method is more mature in application for continental tight clastic rocks in the Sichuan Basin. It has a higher fault tolerance for logging curve environmental impacts. It is more suitable for establishing a full-wellbore pressure profile for the Shaximiao-1 Member with its strong heterogeneity.

$$P_p = \sigma_V - (\sigma_V - P_h)\left(\frac{\Delta t_n}{\Delta t_0}\right)^N \quad (12)$$

4.2 Regional Single-Well Geomechanical Parameter Analysis

(1) Formation Pore Pressure Calculation

After selecting the pore pressure prediction model suitable for this block, based on conventional logging data and using laboratory test and field measured data as calibration points, we predicted the regional pore pressure. Referring to the pressure and temperature of the No. 2 sand group in the 1st sub-member of the Shaximiao-1 Member in the NC002 well area of the study block, the formation pressure is 22.85–24.36 MPa, and the pressure coefficient is 1.10. Taking well NC002-S-H1 as an example, the calculated single-well pore pressure profile is shown in Figure 10.

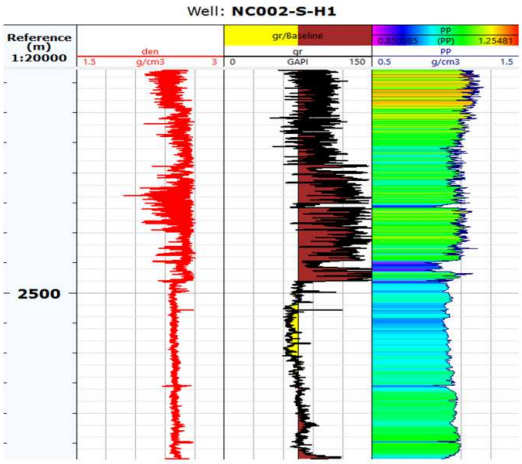

Figure 10. Single-well pore pressure profile for well NC002-S-H12.

(2) Geomechanical Parameter Calculation

Based on conventional logging data and using the laboratory experimental data from the previous section as calibration points, we used Mathcad software for prediction calculation. This obtained the prediction results of single-well geomechanical parameters for the block. We imported the prediction results into logging interpretation software to obtain single-well geomechanical parameter profiles. Due to space limitations, we select well NC002-S-H1 for display, as shown in Figure 11.

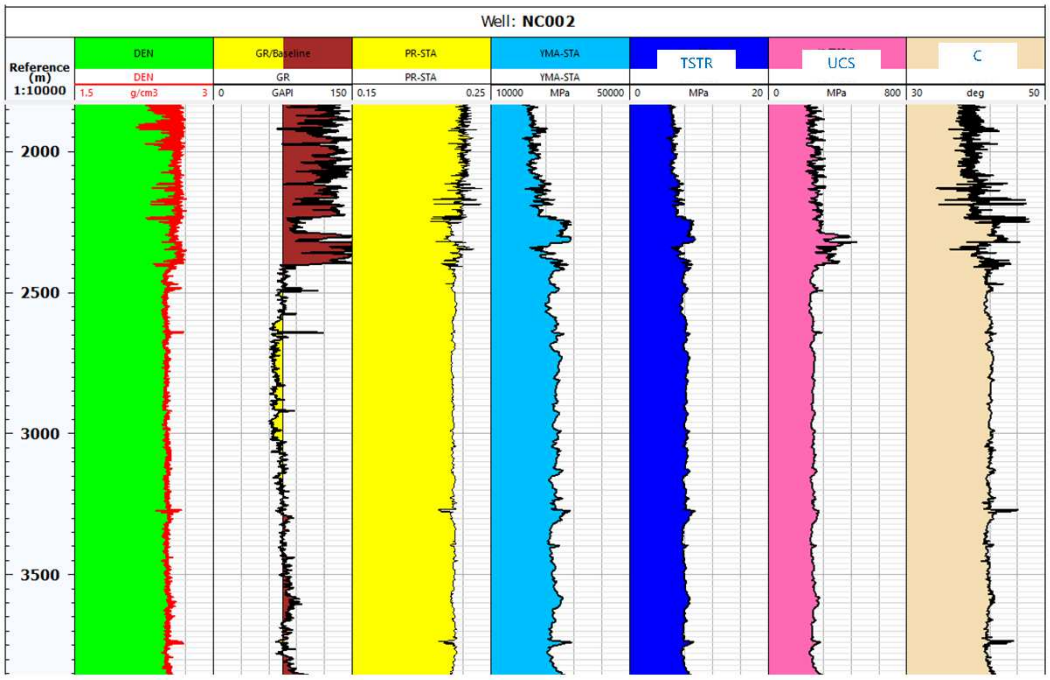

Figure 11. Single-well geomechanical parameter profile for well NC002-S-H1

(3) In-Situ Stress Calculation

Based on logging data and the geomechanical parameters calculated above, and using laboratory tests for calibration. Since the target layer in the study area belongs to a strike-slip stress regime, the closure pressure is approximately equal to the minimum horizontal principal stress. Therefore, we used the pump-off pressure as a reference for calibrating the minimum horizontal principal stress. The calculation results show: For the No. 2 sand group of the Shaximiao-1 Member, the overburden pressure range is between 48–59 MPa; the minimum horizontal principal stress range is between 30–40 MPa; the maximum horizontal principal stress range is between 50–65 MPa. The single-well in-situ stress profile for some target wells is shown in Figure 12.

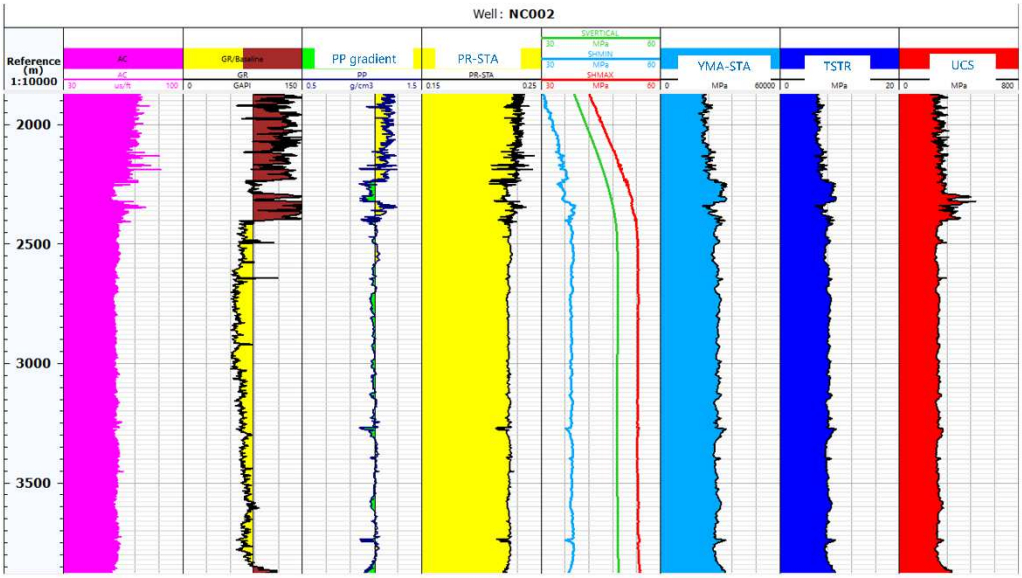

Figure 12. Single-well in-situ stress profile for well NC002-S-H1

4.3 Study on Reservoir 3D Static Geomechanical Parameter Fields

After completing the 3D structural model and 1D geomechanical parameter calculations, we used the regional overall property field establishment method mentioned in the previous chapter. We built 3D static attribute parameter distribution models for geomechanical parameters (elastic modulus, Poisson's ratio, compressive strength, and tensile strength), formation pore pressure, and in-situ stress (vertical in-situ stress, maximum horizontal in-situ stress, and minimum horizontal in-situ stress) of the channel sand bodies in the study area. "Static" means the model is independent of the time dimension. Its core is to characterize the spatial framework and attribute parameter distribution of the geological body at a specific time node (usually the initial state). This is the physical basis and prerequisite for subsequent dynamic numerical simulation.

Figures 13 show the 3D static distribution and vertical/horizontal distribution of elastic modulus, Poisson's ratio, pore pressure gradient, and three-directional in-situ stress for the channel sand

bodies of the No. 2 sand group in the Shaximiao-1 Member of the Shaximiao Formation in the study block.

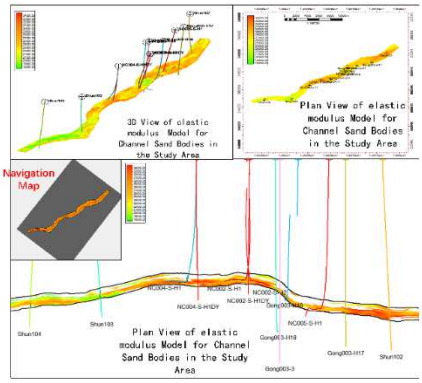

a

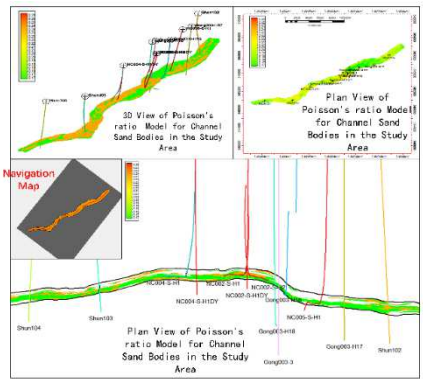

b

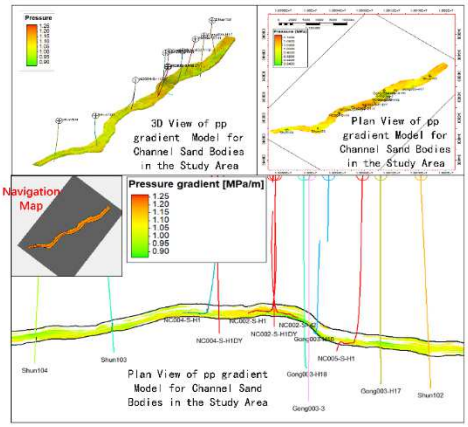

c

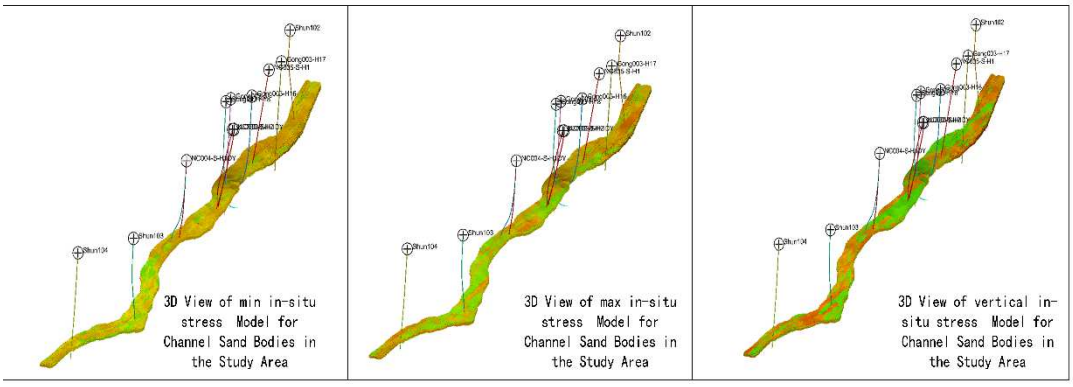

d

Figure 13. Distribution of 3D static geomechanical parameter models (a: Young's modulus; b: Poisson's ratio; c: Pore pressure; d: Three-dimensional in-situ stress profile display)

The elastic modulus of channel sand bodies in the study block ranges from 20 to 34 GPa. Poisson's ratio ranges from 0.17 to 0.25. Pore pressure gradient is around 1.1 g/cm³. For the No. 2 sand group of the Shaximiao-1 Member, the overburden pressure range is between 48–59 MPa; the minimum horizontal principal stress range is between 30–40 MPa; the maximum horizontal principal stress range is between 50–65 MPa.

5 Establishment of Reservoir Geomechanical Model Based on Finite Element Method

5.1 Finite Element Model Establishment

Based on the 3D property parameter field model and geological model, we further establish the geomechanical model. We use the 3D rock mechanical parameter field and pore pressure model as initial conditions. We use the finite element method to numerically simulate the in-situ stress field. This section of the study is based on the VISAGE solver. By setting reasonable tectonic stress boundaries, we conduct forward simulation of the in-situ stress field. This accurately calculates the in-situ stress tensor field within the block. The simulation results include the three principal stress directions and their corresponding in-situ stress magnitudes at each node in the in-situ stress tensor field.

（1）Mesh and Material Property Settings

Based on the mesh model formed by 3D geological modeling of the block, we establish the finite element model mesh. Factors to consider mainly include: boundary loads should be applied uniformly on the model; the model establishment should consider avoiding adverse effects such as stress concentration and thin-plate effects. Therefore, we added lateral meshes three times the original

375 geological model around the original geological model. The outermost layer is wrapped with a 50 m
376 thick rigid plate material. This ensures uniform application of boundary loads on the target block
377 geological model and avoids adverse influencing factors, as shown in Figure 14(a).

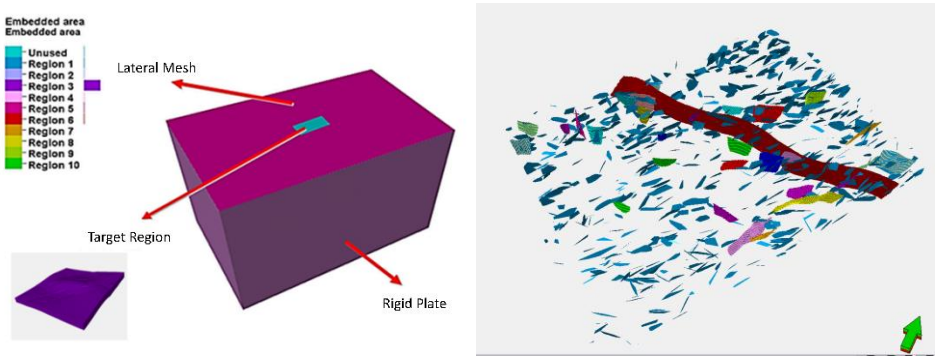

378

379 Figure 14. Schematic diagram of the grid(a: Schematic of Mesh Model, b: Meshes intersected by faults
380 and fractures)

381 After mesh establishment, we need to assign rock mechanical parameters and other data to each
382 mesh. We assign different mechanical properties by region. The outermost 50 m thick rigid plate material
383 does not use a yield criterion. It is given a large Young's modulus to ensure its rigidity. The target block
384 meshes in the middle are assigned properties through the 3D property volume from previous 3D
385 geological modeling. The surrounding rock meshes around them are assigned parameters by outward
386 interpolation based on the target block properties. Meshes intersected by faults are assigned equivalent
387 properties separately. Fault/fracture meshes are shown in Figure 14(b). Fault/fracture properties are
388 shown in Table 2.

389 Table 2. Equivalent materials for faults and fractures

Property	Value
Normal Stiffness	4000 MPa/m
Shear Stiffness	1500 MPa/m
Cohesion	0.001 MPa
Internal Friction Angle	20 deg
Tensile Strength	0.001 MPa
Initial Aperture	0.1m
Fracture Spacing	5m

(2) Boundary Condition Settings

After establishing the finite element model and assigning mechanical properties, we need to determine the boundary conditions of the model. By analyzing the geological situation of the block and the single-well in-situ stress calculation results, we can obtain the in-situ stress gradient for each well. The method for determining the magnitude of boundary loads will use single-well in-situ stress data near the model boundary in the target block as a reference. We convert the single-well in-situ stress data into pressure gradient data. We then calibrate it using experimental data (see Table 3). We also input the three-directional in-situ stress model calculated above as a constraint condition.

Table 3 Experimental test data

Layer	Sample ID	Three-Component Principal Stress Gradients (MPa/m)			In-Situ Stress Orientation
		Maximum Horizontal	Minimum Horizontal	Vertical	Minimum Horizontal
Shaximiao-1 Member	YX-2024-431-06	0.0253	0.0208	0.0228	N 104.2°E

5.2 Analysis of Finite Element Calculation Results

Through the steps of establishing the finite element model, assigning rock mechanical parameter properties, and determining boundary conditions, we established the finite element calculation model for the target block. After solving with the VISAGE solver, we obtained the calculated in-situ stress

magnitude parameter field for the target block, as shown in Figures 15. The VISAGE finite element geomechanical simulation results show that for the channel sand bodies in the study area, the maximum horizontal principal stress is concentrated between 52–60 MPa, the minimum horizontal principal stress is concentrated between 33–42 MPa, and the vertical principal stress is concentrated between 48–58 MPa. The overall variation is small. Maximum horizontal principal stress > vertical principal stress > minimum horizontal principal stress, indicating a strike-slip fault regime.

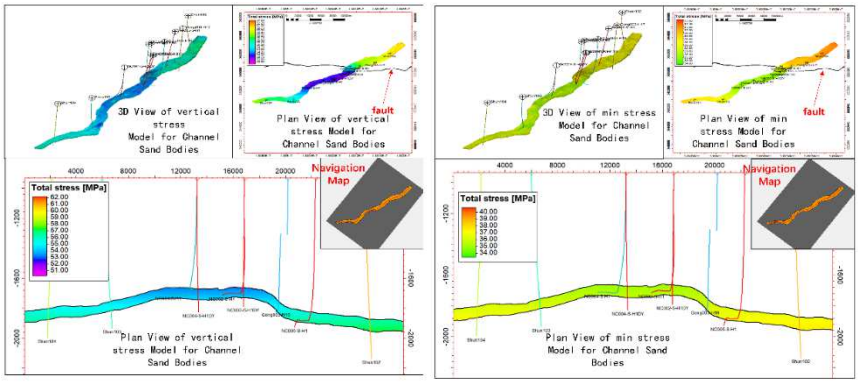

a b

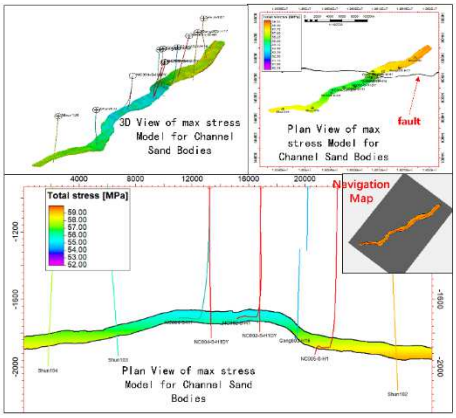

c

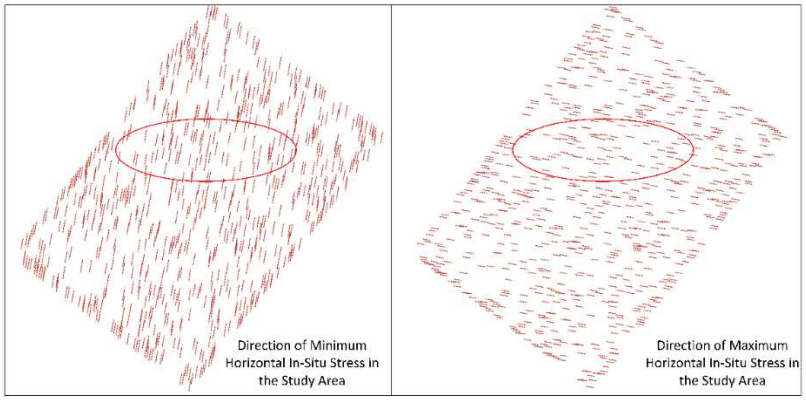

d

Figure 15. In-Situ Stress Parameter Field Model Distribution (a: Vertical In-Situ Stress; b: Maximum Horizontal Principal Stress; c: Minimum Horizontal Principal Stress; d: Horizontal Stress Orientation)

The overall in-situ stress direction is roughly the same as the maximum horizontal principal stress direction indicated by imaging logging. However, local disturbances in direction occur at faults. The in-situ stress magnitude is basically related to burial depth. Faults have a significant segmentation and release effect on in-situ stress distribution. The in-situ stress changes significantly on both sides of the fault. At the same time, the match between the predicted in-situ stress calculation results and the measured in-situ stress values from calibration wells is over 90%, indicating high credibility.

Table 4 Comparison between finite element simulation results and measured values

Value Type	Max. Horizontal Principal Stress (MPa)	Min. Horizontal Principal Stress (MPa)
Finite Element Simulation Value	52.5	33.2
Measured Value (Calibration Well)	57.47	36.04
Match Rate	91.4%	92.1%

6 Results and Discussion

Based on the research concept of "geological engineering integration", this paper uses indoor rock mechanics experiments as the physical support and multi-source data from logging as the constraint conditions. The research scope has been expanded from one-dimensional evaluation of a single well to three-dimensional spatial field simulation. A three-dimensional geological mechanics model of tight sandstone reservoirs has been systematically constructed. The specific research results and discussions are as follows:

6.1The results of the petrographic model and their sedimentary geological significance

The lithofacies model shows that the sand body of the Shangyi section in the study area is distributed in a strip-like pattern on the plane, with certain continuity and branching properties locally, and shows a multi-stage sand body stacking characteristic in the vertical direction. This distribution feature is consistent with the continental river channel sedimentary background of the Shaximiao Formation, indicating that the distribution of the sand body in the study area is mainly controlled by ancient river channel migration, source supply, and sedimentary microfacies combination [QIAO Ling,et al.2013]. Compared with the method of simply dividing sand and mud rocks based on seismic attribute thresholds, the joint modeling of wells and seismic data can simultaneously utilize the high vertical resolution of well logging data and the lateral continuity of seismic data, thereby reducing the uncertainty of sand body prediction between wells. The lithofacies model has a good corresponding relationship with the low-value section of the logging GR and the strong amplitude response of the seismic, indicating that this

model can reasonably depict the spatial boundaries of the river channel sand body and provide geological constraints for the phased simulation of porosity, permeability and rock mechanical parameters.

6.2 Distribution of Reservoir Physical Properties and Factors Controlling Heterogeneity

The three-dimensional physical property model indicates that the porosity of the river channel sand body of the Shangyi section in the study area is mainly 4-8%, the permeability is 0.01-3 mD, and the water saturation is 30-45%. The overall reservoir is a low-porosity, low-permeability - very low-permeability tight sandstone reservoir, which is basically consistent with the understanding that the tight sandstone reservoirs of the Shaximiao Formation in the Sichuan Basin generally have low porosity and low permeability [HUANG Dong,et al.2017]. On the plane, the high porosity and high permeability areas are mainly distributed in strip-like patterns along the direction of the river channel sand body distribution, indicating that the sedimentary microfacies have a first-level control effect on reservoir physical properties [ZHANG Daowei,et al.2022]. The relatively coarse grain size, lower mud content and better original pore structure in the river channel sand body are conducive to the preservation of high porosity and permeability; while the physical properties in the mud sedimentary areas at the edge or floodplain of the river channel or plain deteriorate significantly, reflecting the control of lithology on reservoir quality.

However, the model also shows that the porosity and permeability of the same river channel sand body are not uniformly distributed, but have obvious patch-like and strip-like variations. This indicates that in addition to the sedimentary facies, compaction, cementation, mud filling and local crack development are also factors that affect reservoir physical properties [YAN Xueying,et al.2024]. This understanding is consistent with the research conclusion that the tight sandstone reservoirs of the Jurassic

in the Sichuan Basin generally have strong heterogeneity. For development deployment, identifying favorable areas based solely on sand body thickness or sand-to-ground ratio is limited. It is necessary to comprehensively consider lithofacies, porosity-permeability conditions, water saturation and stress conditions.

Therefore, the overlapping area of high-porosity and high-permeability sand bodies and low water saturation should be selected as the preferred target, while areas with poor porosity-permeability conditions but with developed fractures or favorable stress conditions may also become potential effective reservoirs after fracturing modification.

6.3 Characteristics of Three-Dimensional Geomechanical Parameter Fields and Their Mechanical Significance

The three-dimensional rock mechanics model shows that the Young's modulus, Poisson's ratio, compressive strength and stress parameters of the study area's Shangyi section have obvious non-homogeneity in both the longitudinal and transverse directions, as shown in Figures 16-19. Overall, the Young's modulus of the sandstone section is relatively high, and the Poisson's ratio is low; while the sandstone section shows a low Young's modulus and high Poisson's ratio. This difference is mainly controlled by lithology, mineral composition, mud content and pore structure [WANG B,et al.2020].

In the calculation of horizontal principal stress, the elastic modulus directly participates in the constitutive strain term, so the inter-layer differences of rock mechanics parameters will cause obvious stress stratification in the interbedded sand and mud rock sections. For this reservoir of the Shaximiao Formation with frequent interlayering of river channel sand and mud rock, stress stratification may affect the vertical extension of fracturing cracks, causing the fractures to turn, stagnate or be highly restricted

near the mechanical interface. The pore pressure gradient is approximately 1.1 g/cm³, indicating that the pressure state in the study area is slightly higher than the normal pressure; the pore pressure affects the rock fracture conditions by reducing the effective stress, and has an important influence on the initiation pressure and extension pressure of fractures.

6.4 Simulation Results of Finite Element Stress Field and Regional Stress Mechanism

Based on the three-dimensional geological model and the rock mechanics parameter model, this paper uses the finite element method to simulate the current in-situ stress field in the study area, obtaining the spatial distribution characteristics of the maximum horizontal principal stress, the minimum horizontal principal stress, and the vertical stress. The simulation results show that the in-situ stress field in the study area has obvious inter-layer differences and lateral heterogeneity. There are certain differences in stress magnitude between different rock types, and the difference in elastic parameters between sandstone reservoirs and mudstone interlayers will lead to local stress concentration or release phenomena. Overall, the vertical stress is mainly controlled by burial depth and the density of overlying strata, and increases with the increase in burial depth; the horizontal principal stress is controlled not only by burial depth but also by the structural morphology, boundary loading conditions, rock mechanics properties, and fracture development. The finite element numerical simulation can comprehensively consider the complex structural geometry, rock heterogeneity, and boundary constraint conditions, and is an important method for predicting the three-dimensional in-situ stress field and evaluating the geomechanical properties of reservoirs [WANG B,et al.2020].

From the perspective of regional stress mechanism, the simulation results show that the current stress field in the study area is mainly dominated by horizontal compression, and the direction of the maximum horizontal principal stress is basically consistent with the regional tectonic stress direction. The artificial fracturing fractures generally tend to extend along the direction of the maximum horizontal principal stress. If the simulation results show that the maximum horizontal principal stress is greater than the vertical stress and the vertical stress is greater than the minimum horizontal principal stress, that is, the maximum horizontal principal stress > vertical principal stress > minimum horizontal principal stress, it indicates that the study area is mainly in a strike-slip stress mechanism; if the vertical stress is the largest, that is, the vertical principal stress > maximum horizontal principal stress > minimum horizontal principal stress, it is a normal fault stress mechanism; if the maximum horizontal principal stress is the largest and the minimum horizontal principal stress is greater than the vertical stress, that is, the maximum horizontal principal stress > minimum horizontal principal stress > vertical principal stress, it is an inverse fault stress mechanism. The stress mechanism and the difference in horizontal principal stress have important control effects on the initiation pressure, extension direction, and complexity of the fracture network of hydraulic fractures. A lower horizontal stress difference is conducive to the turning, branching, and communication of artificial fractures with natural fractures, thereby forming a complex fracture network; a higher horizontal stress difference leads to a stronger directional extension of fractures, and the modified volume is relatively limited. Therefore, the finite element in-situ stress field simulation results can provide a basis for predicting the fracturing fracture direction, selecting favorable modification areas, and deploying the trajectory of horizontal wells in the study area.

6.5 Comprehensive Evaluation of Reservoir Geomechanics

Based on the rock mechanics parameter model and the finite element in-situ stress field simulation results, this paper comprehensively analyzes the reservoir geomechanical characteristics and their effects on the fracturing modification effect in the study area. The results show that the tight sandstone reservoirs in the study area have strong heterogeneity, and there are significant differences in Young's modulus, Poisson's ratio, maximum horizontal principal stress, minimum horizontal principal stress, and horizontal principal stress difference between different rock types. The development segments with higher Young's modulus and lower Poisson's ratio usually exhibit better brittle characteristics, which are conducive to the initiation and extension of fractures during fracturing; while the layers with higher mud content or weaker mechanical properties are more likely to exhibit plastic deformation characteristics, which is not conducive to the formation of a complex fracture network. Existing studies have shown that the elastic parameters of the Jurassic tight sandstone in the Sichuan Basin are controlled by mineral composition, pore structure, and diagenesis, and the difference in rock mechanics properties is an important factor affecting the compressibility of the reservoir and the effect of engineering modification [WANG B,et al.2020].

Combining the in-situ stress simulation results, it can be seen that the fracturing effect of the reservoir is not only controlled by rock brittleness, but also closely related to the current in-situ stress state and the difference in horizontal principal stress. The low horizontal principal stress difference area is more conducive to the turning, branching, and communication of artificial fractures with natural fractures, thereby forming a complex fracture network; the high horizontal principal stress difference area has a stronger directional extension of fractures, and the modified volume is relatively limited.

Therefore, the favorable fracturing areas in the study area should be selected preferentially in areas with higher sand body development degree, stronger rock brittleness, lower horizontal principal stress difference, and better reservoir continuity. Relevant fracturing practices have shown that, given the characteristics of discontinuous sand body distribution, strong planar and longitudinal heterogeneity of the tight sandstone gas reservoirs in the western part of the Sichuan Basin, a refined fracturing design should be carried out by considering the geological characteristics of the reservoir, the mechanical properties of the rocks, and the state of in-situ stress, in order to enhance the degree of reservoir modification and the development effect of individual wells [GUO Jianchun,et al.2023]. In summary, the comprehensive evaluation of reservoir geomechanics can provide important references for the evaluation of sweet spots in the study area, the optimization of horizontal well trajectories, and the design of staged fracturing schemes.

Based on the "geology-engineering integration" research concept, this paper uses laboratory rock mechanical experiments as physical support and multi-source logging data as constraints. It expands the research scope from single-well 1D evaluation to 3D spatial field simulation. It systematically builds a 3D geomechanical model for tight sandstone reservoirs. Specific research results and conclusions are as follows:

(1) Established high-precision single-well geomechanical profiles: Aiming at the geological characteristics of strong tectonic compression and frequent sand-mudstone interbedding in the study area, we selected the Eaton method for formation pore pressure prediction. We used the combined spring model to calculate horizontal principal in-situ stress. This effectively solved the shortcomings of

traditional models that did not consider tectonic anisotropy and inter-layer interactions of different lithologies.

(2) Built 3D static geomechanical parameter fields: Based on the 3D structural model and sedimentary facies model, we used multi-source data fusion technology. We established 3D static attribute models covering elastic modulus, Poisson's ratio, pore pressure, and three-directional in-situ stress. This model is not affected by the time dimension. It finely characterizes the spatial heterogeneity of the geological body in its initial state. It provides the necessary geometric framework and parameter basis for subsequent dynamic simulation.

(3) Completed finite element-based in-situ stress field numerical simulation: The VISAGE finite element geomechanical simulation results show that for the channel sand bodies in the study area, the maximum horizontal principal stress is concentrated between 52–60 MPa, the minimum horizontal principal stress is concentrated between 33–42 MPa, and the vertical principal stress is concentrated between 48–58 MPa. The overall variation is small. Maximum horizontal principal stress > vertical principal stress > minimum horizontal principal stress, indicating a strike-slip fault regime. The results show that faults have a significant segmentation and release effect on in-situ stress. The simulated principal stress magnitudes match field measured values with over 90% accuracy, verifying the reliability of the model.

Statements and Declarations

Declaration of Competing Interest

The authors declare that they have no known competing financial interests or personal relationships that could have appeared to influence the work reported in this paper.

Data availability statement

The data that support the findings of this study are available from the corresponding author upon reasonable request.

Author contributions

Qingsong Tang: Methodology, Investigation; Runfeng Shi: Conceptualization, Writing – Original Draft, Data analysis; Zhongbao Wu: Supervision, Writing – Review & Editing, Project administration (Corresponding author); Bing He: Visualization, Validation; Houbin Liu: Validation, Discussion; Benjian Zhang: Resources; Minglei Wang: Validation; Xun Zhu: Data curation; Kai Yu: Investigation; Huizhu Xiang: Visualization. All authors have read and agreed to the published version of the manuscript.

References

1. CHEN Ke, YU Zhihao, WANG Shouyi, et al. Shale fracture network propagation simulation in non-uniform stress field near fault [J]. Fault-Block Oil & Gas Field, 2023, 30(02): 213–221.
2. CHEN Ming, YU Liwen, QIN Rui, et al. A new method for prediction of pore pressure in shale formation [J]. Complex Hydrocarbon Reservoirs, 2021, 14(03): 27–30+69.
3. FAN Yu, YU Xingchuan, GUO Jianhua, et al. Vertical distribution law of formation pressure in Penglai gas area in Sichuan Basin [J]. Petroleum Geology & Oilfield Development in Daqing, 2023, 42(02): 59–67.
4. GUO Jianchun, LU Qianli, LIU Zhuang, et al. Concept and key technology of "multi-scale high-density" fracturing technology: A case study of tight sandstone gas reservoirs in the western Sichuan Basin[J]. Natural Gas Industry, 2023, 43(2): 67-76.

5. HUANG Dong, YANG Yueming, YANG Guang, et al. Countermeasure and progress of exploration and developmentof Jurassic tight oil in the Sichuan Basin [J]. Petroleum Geology and Experiment, 2017, 39(03): 304–310.
6. HUANG Rongzun. Initiation and propagation of hydraulic fracturing fractures[J]. Petroleum Exploration and Development, 1981, (05): 62–74.
7. JIA Lichun, LI Zhuzheng, CHEN Liping. Pore pressure prediction for fractured carbonate formation in Central Sichuan Based on Effective Stress Principle [J]. Drilling & Production Technology, 2023, 46(05): 93–99.
8. JIANG Xiaohong, SUN Liang, CHEN Jianchuan, et al. Establishment and application of three-pressure profile in GM block , Sichuan gasfield[J]. Natural Gas Exploration and Development, 2016, 39(01): 57–59+62+13–14.
9. LI Xiuming, LIU Zhigang, YAN Xiaowei, et al. Effect on the identification ability of channel sand bodies and faults for shot channel density degradation of observation system:an example of GSM high-density 3D observation system for the seismic exploration in Shaximiao Formation,Central Sichuan [J]. Mineral Resources and Geology, 2022, 36(03): 630–639.
10. LIAO Guangzhi, TANG Qingsong, WANG Minglei, et al. Making Greater Efforts for Oil Exploration and Production for the Long Term Boom of Crude Oil in Sichuan Basin [J]. Oil Forum, 2025, 44(03): 1–11.
11. LIU Qiming, ZHU Tiedong, CHEN Hanjun. Application of three-pressure profile calculation to complex situation prevent and treatment in Pengzhou Gas Field, the Sichuan Basin [J]. Natural Gas Exploration and Development, 2017, 40(04): 101–104.
12. LIU Ying. TTriple-Pressure Prediction and Borehole Wall Stability Analysis of Continental Shale Formation [J]. Journal of Jianghan Petroleum University of Staff and Workers, 2021, 34(05): 5–7.

13. QIAO Ling. Study on favorable block evaluation for oil and gas exploration in the Da'anzhan Member of Jurassic in central Sichuan[D]. Chengdu: Southwest Petroleum University, 2013.
14. Stein Inge Pedersen. Automatic Fault Extraction Using Artificial Ants[C]//2002 SEG Annual Meeting. 2002.
15. WANG Xiuchao. Application of Geo-Stress Prediction in the Dazhai Shale Gasfield of Southern Sichuan [J]. Special Oil & Gas Reservoirs, 2018, 25(05): 35–38.
16. Wang B,Chen X Z,Chen J,et al.2020.Elastic characteristics and petrophysical modeling of the Jurassic tight sandstone in Sichuan Basin Chinese J.Geophys.（in Chinese）,63（12）:4528—4539
17. YANG Yu, XIE Jirong, CAO Zhenglin, et al. Forming conditions and key technologies for exploration and development of large tight sandstone gas reservoirs in Shaximiao Formation, Tianfu gas field of Sichuan Basin [J]. Acta Petrolei Sinica, 2023, 44(06): 917–932.
18. YAN Xueying, SANG Qin, JIANG Yuqiang, et al. Main controlling factors for the high yield of tight oil in the Jurassic Da'anzhai Section in the western area of Gongshanmiao,Sichuan Basin [J]. Lithologic Reservoirs, 2024, 36(06): 98–109.
19. ZHANG Daowei, YANG Yu. Exploration potential and development direction of continental tight sandstone gas in the Sichuan Basin [J]. Natural Gas Industry, 2022, 42(01): 1–11.
20. ZHAO Xuyang, GUO Haimin, LI Zixuan, et al. Modeling of in-situ stress field and rock mechanics parametersbased on logging shear wave prediction [J]. Fault-Block Oil & Gas Field, 2021, 28(02): 235–240.